Celestial Mech Dyn Astr (2007) 97:165–187
DOI 10.1007/s10569-006-9059-0

ORIGINAL ARTICLE

# ISA accelerometer onboard the Mercury Planetary Orbiter: error budget

**Valerio Iafolla · David M. Lucchesi · Sergio Nozzoli · Francesco Santoli**

Received: 11 May 2006 / Revised: 23 October 2006 / Accepted: 5 December 2006 /
Published online: 9 February 2007


**Abstract** We have estimated a preliminary error budget for the Italian Spring Accelerometer (ISA) that will be allocated onboard the Mercury Planetary Orbiter (MPO) of the European Space Agency (ESA) space mission to Mercury named BepiColombo. The role of the accelerometer is to remove from the list of unknowns the non-gravitational accelerations that perturb the gravitational trajectory followed by the MPO in the strong radiation environment that characterises the orbit of Mercury around the Sun. Such a role is of fundamental importance in the context of the very ambitious goals of the Radio Science Experiments (RSE) of the BepiColombo mission. We have subdivided the errors on the accelerometer measurements into two main families: (i) the pseudo-sinusoidal errors and (ii) the random errors. The former are characterised by a periodic behaviour with the frequency of the satellite mean anomaly and its higher order harmonic components, i.e., they are deterministic errors. The latter are characterised by an unknown frequency distribution and we assumed for them a noise-like spectrum, i.e., they are stochastic errors. Among the pseudo-sinusoidal errors, the main contribution is due to the effects of the *gravity gradients* and the *inertial forces*, while among the random-like errors the main disturbing effect is due to the MPO *centre-of-mass displacements* produced by the onboard High Gain Antenna (HGA) movements and by the fuel consumption and sloshing. Very subtle to be considered are also the random errors produced by the MPO attitude corrections necessary to guarantee the nadir pointing of the spacecraft. We have therefore formulated the ISA error budget and the requirements for the satellite in order to guarantee an orbit reconstruction for the MPO spacecraft with an along-track accuracy of about

V. Iafolla (✉) · D. M. Lucchesi · S. Nozzoli · F. Santoli
Istituto di Fisica dello Spazio Interplanetario, IFSI/INAF,
V. Fosso del Cavaliere, 100, 00133 Rome, Italy
e-mail: valerio.iafolla@ifsi-roma.inaf.it

D. M. Lucchesi
Istituto di Scienza e Tecnologie della Informazione, ISTI/CNR,
Via Moruzzi, 1, 56124 Pisa, Italy

1 m over the orbital period of the satellite around Mercury in such a way to satisfy the RSE requirements.

**Keywords** Solar system · Mercury · Accelerometers · Artificial satellites · Perturbations · Gravimetry · General relativity

## 1 Introduction

The BepiColombo mission to Mercury aims to perform a detailed study of the innermost planet of our solar system in order to obtain a deeper knowledge on Mercury's internal structure, chemical composition and the nature of its (apparently) very small dipole magnetic field (see Grard and Balogh 2001; Spohn et al. 2001). Among the several experiments that will be performed, the Radio Science Experiments (RSE) will be in charge of three experiments intimately related to each other: (i) a gravimetry experiment, (ii) a rotation experiment and (iii) a general relativity experiment. A spacecraft, the Mercury Planetary Orbiter (MPO), will be placed in orbit around Mercury for a nominal mission of one terrestrial year.[1]

The outcome from the cited experiments is to improve significantly our present knowledge on Mercury's gravity field and local anomalies, its rotational state and on the heliocentric orbit of the planet centre-of-mass around the Sun. See Milani et al. (2001, 2002) for further details.

The MPO spacecraft will be tracked from Earth-ground-stations[2] with ultra-stable and multi-frequency radio links. Indeed, for the first time, an interplanetary spacecraft will be tracked with a multi-frequency coherent link, both in range and range-rate. These links will be in the *X(up)/X(down), X(up)/Ka(down)* and *Ka(up)/Ka(down)* bands. An onboard High Gain Antenna (HGA) will be used as the main link antenna to Earth during the science phase.

The high performance of the tracking from Earth will allows for a very good estimate of Mercury's gravity field as well as for the heliocentric orbit of the planet centre-of-mass. The gravity field coefficients with degree $\ell = 2$ are sensitive to the planet moments of inertia differences. Hence, their knowledge, together with the results of the rotation experiment (whose relevant parameters are still sensitive to Mercury's moments of inertia differences), will allow for the determination of Mercury's internal structure. The rotation of Mercury, with the 2:3 resonance between the rotation period and the revolution period of the planet (Colombo 1965, 1966; Colombo and Shapiro 1966), was firstly measured with Doppler radar. The goal of the RSE of BepiColombo are a better measurement of the obliquity of Mercury's equator with respect to its orbital plane and a better measurement of the libration in longitude induced by the nominal resonant rotation with the period of one Mercury year (about 88 terrestrial days).

We refer to Milani et al. (2001, 2002) for a detailed discussion of the results of a numerical simulation for the gravimetry and rotation experiments and of the relativity experiment, while we refer to Iess and Boscagli (2001) for the characteristics of the tracking system (on ground and onboard) necessary to perform the goals of the BepiColombo RSE.

[1] The launch epoch for the mission is expected in August 2013 with a Soyuz 2-lB/Fregat M, while the insertion of the MPO around Mercury is expected in August 2019.

[2] At least one of the Deep Space Network (DSN).

Because of the higher frequencies and plasma compensation technique and because of the independence from the surface topography characteristics (the planet centre-of-mass will be equivalent to the traditional radar bounce point), the ephemeris of the new orbit of Mercury will be much more accurate than the present one, and this will allow (together with the propagation of the electromagnetic waves) a very accurate general relativity experiment.

It is clear that, in order to reach the ambitious objectives of the RSE, it is necessary to reconstruct *a posteriori* the "pure" gravitational orbit of the MPO and then the *geodesic* of Mercury's centre-of-mass around the Sun. For these reasons, among the instruments to be placed onboard the MPO in the context of the RSE there will be an accelerometer whose measurements will be used a posteriori in order to remove the non-gravitational accelerations from the right hand side of the equations of motion in such a way to obtain the gravitational trajectory followed by the spacecraft in the strong radiation environment of Mercury, i.e., in order to separate the gravitational and the non-gravitational effects.

The mathematical formula which approximates the measurements of an accelerometer is:

$$\vec{A}_{\mathrm{mes}} \cong \vec{B} + S_{\mathrm{f}}\vec{A}_{\mathrm{true}} + \vec{A}_{\mathrm{noise}} \tag{1}$$

where $\vec{A}_{\mathrm{mes}}$ and $\vec{A}_{\mathrm{true}}$ are the measured acceleration and the true acceleration on the accelerometer proof-mass, $\vec{B}$ and $S_{\mathrm{f}}$ are the proof-mass bias and scale factor, finally $\vec{A}_{\mathrm{noise}}$ represents the resultant acceleration due to stochastic perturbations on the proof-mass. In Eq. 1 we omitted possible non-linear contributions to the accelerometer measurements. The bias and the scale factor will be determined as two unknowns by an infligth calibration during a precise orbit determination. The bias estimate is a critical point. Indeed, one point is related with how the bias can change with time and how it can reflect the existence of residuals systematic effects due to thermal effects, in particular at very long periods. We refer to Milani et al. (2001) and Lucchesi and Iafolla (2006) for major details. Equation 2 below gives the true accelerations acting on the accelerometer proof-mass.

$$\vec{A}_{\mathrm{true}} = (\vec{\nabla}\cdot\vec{g})\,\vec{R} - \vec{\omega}\wedge(\vec{\omega}\wedge\vec{R}) - \dot{\vec{\omega}}\wedge\vec{R} - 2(\vec{\omega}\wedge\dot{\vec{R}}) - \vec{A}_{\mathrm{NGP}} \tag{2}$$

where $\vec{R}$ represents the proof-mass position with respect to the spacecraft centre-of-mass (COM), $\vec{g}$ is the gravitational acceleration on the spacecraft COM, $\vec{\omega}$ and $\dot{\vec{\omega}}$ are, respectively, the angular rate and angular acceleration of the MPO, hence the middle terms are the centrifugal acceleration, the angular acceleration and the Coriolis acceleration; finally $\vec{A}_{\mathrm{NGP}}$ represents the resultant linear acceleration due to the non-gravitational perturbations (NGP) acting on the accelerometer, i.e., the objective of the accelerometer measurements. Equations 3 and 4 describe, respectively, the impact of the gravity gradients and of the inertial accelerations on the accelerometer measurements:

$$\vec{a}_{gg} = \begin{pmatrix} a_{ggX} \\ a_{ggY} \\ a_{ggZ} \end{pmatrix} = \begin{pmatrix} 2n^2\left(\frac{a}{r}\right)^3 & 0 & 0 \\ 0 & -n^2\left(\frac{a}{r}\right)^3 & 0 \\ 0 & 0 & -n^2\left(\frac{a}{r}\right)^3 \end{pmatrix} \begin{pmatrix} \Delta X \\ \Delta Y \\ \Delta Z \end{pmatrix} \tag{3}$$

$$\vec{a}_{app} = \begin{pmatrix} a_{appX} \\ a_{appY} \\ a_{appZ} \end{pmatrix} \begin{pmatrix} \omega_0^2 & \dot{\omega}_0 & 0 \\ -\dot{\omega}_0 & \omega_0^2 & 0 \\ 0 & 0 & 0 \end{pmatrix} \begin{pmatrix} \Delta X \\ \Delta Y \\ \Delta Z \end{pmatrix} \tag{4}$$

where $n$ ($\cong 7.52 \cdot 10^{-4}$ rad/s) and $a$ ($\cong 3389$ km) are, respectively, the MPO mean motion around Mercury and its semi-major axis connected through Kepler third law ($n^2a^3 = GM_\mathrm{m}$),[3] $r$ represents the spacecraft distance with respect Mercury's COM. The quantities $\omega_0$ and $\dot{\omega}_0$ are, respectively, the nominal values of the MPO angular rate and angular acceleration because of the demanded nadir pointing of the spacecraft. Finally, $\Delta X, \Delta Y, \Delta Z$ are the components of the accelerometer proof-mass position with respect to the satellite COM, i.e., of the vector $\vec{R}$ previously introduced.

Therefore, while $\vec{A}_\mathrm{NGP}$ represents the true goal of the accelerometer measurements, the other terms from Eq. 2 contributing to the accelerometer readings, are systematic effects that must be removed from the measurements or kept below a given threshold, in agreement with the RSE requirements on the accelerometer measurement error.

The Italian Spring Accelerometer (ISA) has been considered and then selected by the European Space Agency (ESA) to fly on-board the MPO. The NGP are critical for the RSE, especially the disturbing effects produced on the MPO orbit by the incoming visible solar radiation pressure, the largest NGP.

In three previous papers have been described: (i) the ISA accelerometer intrinsic characteristics (see Iafolla and Nozzoli 2001), (ii) then ISA implementation onboard the MPO (see Iafolla et al. 2004), (iii) finally the impact of the NGP on the MPO orbit, both in their long-period and short-period effects, and the advantages of an onboard accelerometer with respect to the best modelling of the NGP (see Lucchesi and Iafolla 2006). In the last paper, the issue of the inflight calibration of the accelerometer has been introduced. However, a forthcoming paper will be devoted to this very complex aspect.

In the present paper, we are interested to address the results of our preliminary error budget for the ISA accelerometer, with special care of the errors due to the gravity gradients and inertial accelerations, as well as for the noise due to the angular rate and angular acceleration corrections necessary to guarantee the nadir pointing of the MPO spacecraft.

The rest of the paper is organised as follows. In Sect. 2, we recall the orbit configuration of the MPO and the main characteristics of ISA that will be used in the subsequent sections. In Sects. 3 and 4, we focus on the error budget estimate from the main disturbing effects characterised by a periodic behaviour. Among these errors are those from the gravity gradients and inertial accelerations because of the finite dimensions of the ISA accelerometer and the non-perfect coincidence between ISA centre-of-mass and the MPO one. In Sect. 5, we introduce our estimate of the error budget produced by the random effects, like those due to the angular rate and angular acceleration corrections necessary to guarantee the nadir pointing of the spacecraft. Finally, in Sect. 6, the conclusions and recommendations are drawn.

## 2 The MPO orbit and ISA characteristics

In this section we are interested to recall the main characteristics of the MPO spacecraft and of the ISA accelerometer that are useful for the arguments developed in the subsequent sections. The MPO spacecraft will be a 3-axis stabilised satellite (nadir pointing), characterised by a $400 \times 1500$ km polar orbit around Mercury. In Table 1 are shown the main orbital parameters of the MPO. This orbit configuration is suitable

[3] With $G$ the gravitational constant and $M_\mathrm{m}$ Mercury's mass.

**Table 1** The MPO main orbital parameters

| Orbital parameter | Symbol | Numerical value |
|---|---|---|
| Semi major axis | $a$ | 3389 km |
| Eccentricity | $e$ | 0.162 |
| Inclination | $I$ | 90° |
| Orbital period | $P$ | 8355 s |

for the recovery, with a signal-to-noise ratio larger than 10, of Mercury's gravity field up to degree $\ell = 25$ and of its gravity anomalies with a spatial resolution of about 300 km at the same degree $\ell = 25$ (see Milani et al. 2001).

In order to reach the ambitious goals of the RSE, it is necessary an accuracy in the along-track orbit reconstruction of about 1 m (see Milani et al. 2001) over one orbital revolution of the MPO around Mercury, i.e., over 8355 s. This corresponds to an along-track acceleration accuracy of about $10^{-8}\,\mathrm{m/s^2}$. Therefore, this number has been considered equivalent to the accelerometer measurement error over the typical arc length during one observation session from Earth's ground antenna(s).

In fact, as we underlined in the Introduction, the key role of an onboard accelerometer is to remove (a posteriori) from the list of unknowns the non-gravitational accelerations that perturb the MPO orbit. In particular, the direct solar radiation pressure produces the largest effects on the MPO orbit because of its proximity to the Sun.

The acceleration produced by the direct solar radiation pressure on a spherical satellite is:

$$a_{\mathrm{Sun}} = -C_R \frac{A\Phi_{\mathrm{Sun}}}{mc}\left(\frac{\bar{R}_{\mathrm{Sun}}}{R_{\mathrm{Sun}}}\right)^2 \hat{S} \tag{5}$$

where $C_{\mathrm{R}}$ represents the satellite radiation coefficient ($\approx 1$), $A/m$ its area-to-mass ratio, $c$ the speed of light, $\Phi_{\mathrm{Sun}}$ the solar irradiance at the average distance $\bar{R}_{\mathrm{Sun}}$ of Mercury from the Sun, and $\hat{S}$ represents the unit vector towards the Sun. The last squared term is due to the modulation coming from the large eccentricity of Mercury's orbit around the Sun (about 0.206).

As a consequence of the extreme variations of the solar irradiance over Mercury's orbit,[4] the disturbing acceleration due to the direct solar radiation varies in the range between $4 \cdot 10^{-7}\,\mathrm{m/s^2}$ and $1 \cdot 10^{-6}\,\mathrm{m/s^2}$ (i.e., it is up to 2 orders-of-magnitude larger than the requested mission accuracy). We refer to Lucchesi and Iafolla (2006) for further details.

The Italian Spring Accelerometer (ISA) has been selected by ESA to fly on-board the MPO. ISA is a three-axis torsional oscillators (Iafolla and Nozzoli 2001) with an intrinsic noise of $9.8 \cdot 10^{-10}/\sqrt{\mathrm{Hz}}$ in the frequency band of $3 \cdot 10^{-5}$to$10^{-1}$ Hz. As described in Milani et al. (2001), the typical arc length will be about 8 h.[5] Therefore, this value has been assumed as the lower limit of the accelerometer bandwidth

[4] We assumed, for the sake of simplicity, the MPO spherical in shape and with the same area-to-mass ratio of the planned spacecraft (about $1.9 \cdot 10^{-2}\,\mathrm{m^2/kg}$) corresponding to a mass of approximately 357 kg.

[5] Between 4 and 12 h depending on the visibility conditions. The visibility conditions constrain the way in which the data are collected in the case of range and range-rate measurements, which will not be continuous.

(about $3 \cdot 10^{-5}$ Hz). The upper limit for the bandwidth is dictated by the response of the accelerometer to a given perturbation that must be linear. This means that the accelerometer must be used in a frequency region where its transfer function is flat, i.e., below the proof-mass resonance frequency.

The intrinsic noise level of ISA is given in unit of $\sqrt{\text{Hz}}$. This means that over a time interval $\Delta t$—whose value is to be considered inside the accelerometer bandwidth—the accelerometer performances are better than $10^{-8}\,\text{m/s}^2$, that is of the accuracy required by the RSE for the MPO orbit reconstruction.

Because, as underlined in the Introduction, we are interested in the error budget produced by two kind of errors: (i) the periodic or pseudo-sinusoidal errors, and (ii) the random-like errors, in the following we will describe their contribution in terms of what we define as the accelerometer accuracy $A_0 = 9.8 \cdot 10^{-9}\,\text{m/s}^2$ and the accelerometer spectral density $\left(S_0 = 9.8 \cdot 10^{-9}\,\text{m/s}^2/\sqrt{\text{Hz}}\right)$.

Indeed, the pseudo-sinusoidal errors are characterised by a clear periodic contribution and show their effects over the MPO orbital period. Hence, they are suitable to be described by the acceleration accuracy over the spacecraft orbital period or, more in general, over the arc length. Instead, the random-like terms have not a clear frequency content (they are spread inside the accelerometer bandwidth) and are more properly characterised by a noise-like spectrum, therefore they are more suitable to be described in terms of acceleration per unit of $\sqrt{\text{Hz}}$.

However, it is not necessary to retain a spectral density of $9.8 \cdot 10^{-8}\,\text{m/s}^2/\sqrt{\text{Hz}}$ through all the accelerometer's bandwidth. Indeed, as shown in Fig. 1, which describes the noise due to the accelerometer and tracking system, at low frequency the noise is dominated by the thermal disturbing effects while at higher frequencies the noise is dominated by the tracking errors [ESA 2006]. In the figure the dashed-dot line represents ISA intrinsic noise; the solid line represents the thermal noise effects due to a possible white noise at a level of $4°\text{C}/\sqrt{\text{Hz}}$, which may be present at the

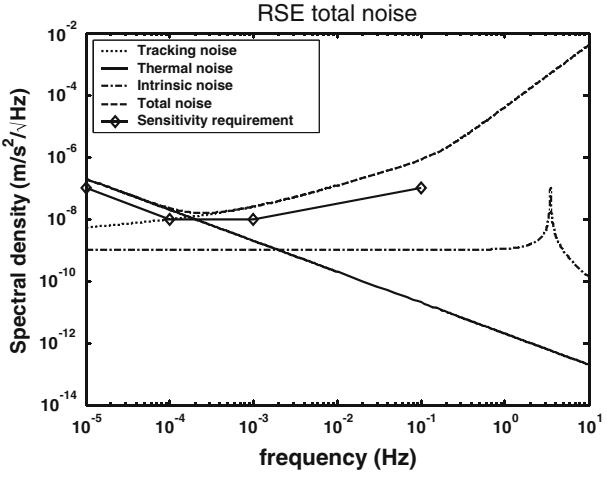


**Fig. 1** Total noise coming from the accelerometer and to the tracking as used in the simulations that have been performed to prove the reliability of the RSE (ESA 2006). This noise level is principally due to the thermal effects on the accelerometer at low frequencies and to the tracking noise at high frequencies

mechanical interface between the spacecraft structure and ISA; the dot line represents the total noise for the tracking reported in acceleration; finally, the dashed line represents the total noise (quadratic sum of the previous noise sources) while the diamond line represents the sensitivity requirement. We stress that these results have been obtained in the case of a passive thermal control. Because an active thermal control will be used as baseline, the thermal effects will be further attenuated by a factor 700, see below in the text.

From the total noise level shown in Fig. 1 there has been constructed the reference level for the ISA performances used in the error budget analysis developed in the next sections. Therefore, we need to fully exploit the accelerometer performances only in a narrower bandwidth, between $10^{-4}$ Hz and $10^{-3}$ Hz. We also underline that in such a Figure, the contribution of all the errors which are the subject of the present discussion it is not indicated.

The impact of unmodelled thermal effects on the accelerometer readings may cause systematic errors in the results of Mercury's gravity field coefficients determination as well as in the estimate of the relativistic parameters (Milani et al. 2001, 2002). The thermal effects appear both on long time scales, at the revolution period of Mercury (about 88 days) and at half of this period, and on shorter time scales, at the MPO orbital period (8355 s). The former are at very low frequency, outside the accelerometer bandwidth, and will produce (if not properly accounted for) a bias and a slope in the accelerometer readings during the orbit fit (i.e., over each arc observing session). The latter are inside the accelerometer bandwidth and will superimpose and mix with other periodic disturbing effects as well as with the non-gravitational accelerations.

In fact, an accelerometer behaves also like a thermometer, which transforms a temperature variation in an equivalent acceleration. The experimental value of ISA thermal stability is about $5{\cdot}10^{-7}$ m/s$^2$/°C, that is 1°C of variation of the proof-mass temperature produces an equivalent acceleration of about $5{\cdot}10^{-7}$ m/s$^2$ along its sensitive axis.

Therefore, in order to avoid these effects, an active thermal control will be used to attenuate their impact on the accelerometer measurements.[6] The experimental activity performed in our laboratory has presently produced an attenuation factor of about 700, both at the Mercury revolution period and at the MPO orbital period.

The temperature variations (peak-to-peak) estimated for the thermal effects are about 25°C in the case of the long-period effects and about 4°C in the case of the effects at MPO orbital period (ESA 2004a). For instance, in the case of the long-period effect at half of Mercury's year we obtain an unmodelled impact on the accelerometer readings of about:

$$A_{\text{ther}}|_{\text{LP}} \approx 12.5^{\circ}\text{C} \cdot 5 \cdot 10^{-7}\,\text{m/s}^2/^{\circ}\text{C} \cdot \frac{1}{700} = 8.9 \cdot 10^{-9}\,\text{m/s}^2 \tag{6}$$

that is about 91 % of the accelerometer accuracy. However, it is important to stress that our experimental value for the attenuation (about a factor 700) is more than enough in order to satisfy the RSE goals. Indeed, from the simulations of the gravimetry and relativity experiments it has been proved that it is sufficient an attenuation of a factor 100 of the long-period thermal effects in order to guarantee the ambitious objectives of the RSE.

The accelerometer axes are aligned with the Gauss co-moving reference frame, that is the $X$-axis is along the radial direction (from Mercury centre-of-mass to the

[6] Moreover, three thermometers will be used to measure the temperature behaviour for each proof-mass of the accelerometer during the space mission life.

MPO one), the $Y$-axis is along the transversal direction (in the orbital plane) and the $Z$-axis (coincident with the MPO rotation axis) is along the out-of-plane direction. Therefore, for our error budget estimate, we need an accelerometer measurement error along each of these axes smaller than the accelerometer accuracy $A_0$, in the case of the periodic errors, and smaller than the accelerometer spectral density $S_0$, in the case of the random-like errors.

As we underlined above, in order to reconstruct the MPO orbit we are mainly interested to the along-track component, $a_{\mathrm{AT}}$, of the perturbing acceleration. This acceleration is tangential to the MPO elliptical orbit and is obtained by projecting the transversal component and the radial component of the acceleration along the tangent to the MPO orbit.

The (possible) maximum error in the along-track component is given by[7]

$$\Delta a_{\mathrm{ATmax}} = \sqrt{1 - e^2}\,\Delta a_{\mathrm{Tmax}} + e\,\Delta a_{\mathrm{Rmax}} \tag{7}$$

where $\Delta a_{\mathrm{T}}$ and $\Delta a_{\mathrm{R}}$ are, respectively, the errors in the transversal and radial components of the perturbing acceleration while $e$ is the MPO orbit eccentricity. Therefore, the error in the radial component is de-multiplied by the spacecraft eccentricity and it is reduced by about a factor 10, instead the error in the transversal component remains almost unchanged.

In the following sections we will describe our error budget estimate as produced by the main periodic and random error sources on the accelerometer proof-masses.

## 3 Gravity gradients and inertial forces

One of the results of the work developed in Iafolla et al. (2004) was the determination of the best geometrical configuration for the three proof-masses of ISA in order to reduce, as much as possible, the impact of some (not desired) signals on the accelerometer measurements. We are talking about true signals on ISA proof-masses that produce a displacement of the spacecraft centre-of-mass. In Sect. 1 we have defined these signals (as those due to the gravity gradients and the inertial accelerations) as systematic effects on the accelerometer measurements. Therefore, these systematic effects are "false" signals with respect to the accelerometer goal, i.e., the measurement of the non-gravitational accelerations on the MPO.[8] Indeed, these signals may corrupt the correct determination of the non-gravitational accelerations from the measurements of the accelerometer and consequently their removal from the list of unknowns in order to reconstruct the gravitational orbit of the MPO spacecraft.

Because an accelerometer does not measure absolute accelerations (but only differential ones), such disturbing signals are related with varying effects. The most important ones are those connected with the gravity gradients effects of Mercury's gravitational field and those due to the MPO rotation because of the requested nadir pointing, i.e., the effects due to the inertial forces. Therefore, we must be either able to evaluate and then remove such accelerations from the readings of the accelerometer, or to keep them below a specific limit connected with the accelerometer accuracy over the arc length.

[7] This is in reality a quite pessimistic assumption.

[8] These "false" signals are anyway evaluated during the orbit determination and analysis of the MPO orbit around Mercury.

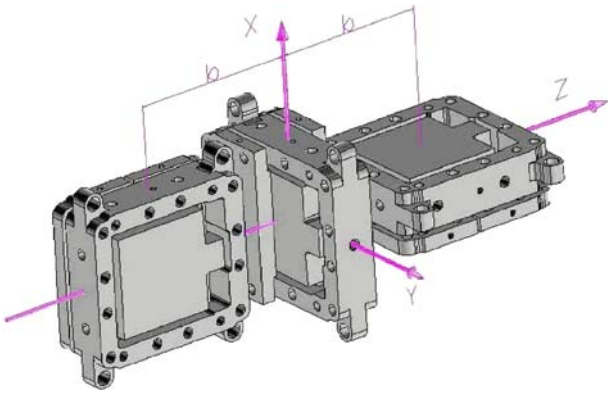


**Fig. 2** ISA geometrical configuration inside the MPO spacecraft. The three centres-of-mass of the three sensitive elements of the accelerometer are aligned along the MPO rotation axis and with ISA centre-of-mass (that of the central element) coincident with the spacecraft (nominal) centre-of-mass. The sensitive axis of the central element is aligned with the MPO rotation axis (along the out-of-plane direction), while the sensitive axes of the other elements (5 cm above or below the accelerometer centre-of-mass) are aligned, respectively, along the radial direction and along the transversal direction. Hereinafter, we will refer to such sensitive elements as the $Z$-element, the $X$-element and the $Y$-element, respectively

The best solution for the accelerometer allocation inside the MPO, taking into account that ISA is composed of three independent torsional harmonic oscillators with sensitive axes perpendicular to each of the "flat" sensitive elements that constitute the accelerometer, is the one shown in Fig. 2. That is, the three sensitive elements are aligned with their centre-of-mass along the MPO rotation axis and with ISA centre-of-mass coincident with the (*nominal*) centre-of-mass of the spacecraft.[9] This solution is obvious, in the sense that it minimises the impact of both the gravity gradients (the accelerometer is close as well as possible to the spacecraft centre-of-mass) and the inertial forces (the sensitive elements are aligned along the MPO rotation axis).

From the mathematical point of view the explanation of such configuration follows from Eq. 8. Indeed, the disturbing accelerations along each sensitive axis of the accelerometer, due to the sum of the gravity gradients and the inertial forces, are:

$$\vec{A}_{\mathrm{PSE}} = \begin{pmatrix} A_X \\ A_Y \\ A_Z \end{pmatrix} = n^2 \begin{pmatrix} \left(3 + 5e^2 + 10e\cos M + 16e^2\cos 2M\right)\Delta X_X \\ -\left(2e\sin M + 5e^2\sin 2M\right)\Delta X_Y \\ \left(2e\sin M + 5e^2\sin 2M\right)\Delta Y_X \\ +\left(\frac{1}{2}e^2 + e\cos M + \frac{5}{2}e^2\cos 2M\right)\Delta Y_Y \\ -\left(1 + \frac{3}{2}e^2 + 3e\cos M + \frac{9}{2}e^2\cos 2M\right)\Delta Z_Z \end{pmatrix} \tag{8}$$

where $n$, $e$ and $M$ are, respectively, the MPO mean motion, orbital eccentricity and mean anomaly (i.e., $\dot{M} = n$). The vectors $\vec{R}_\varsigma = (\Delta_{\varsigma X}, \Delta_{\varsigma Y}, \Delta_{\varsigma Z})$[10] (with $\varsigma = X, Y, Z$), one for each of ISA sensitive axes, represent the displacement of the centre-of-mass for each of the accelerometer sensitive elements with respect to the spacecraft centre-of-mass (COM).

[9] With the term nominal we mean the position of the spacecraft centre-of-mass as determined by the industry neglecting its variations because of the fuel consumption (and sloshing) and the High Gain Antenna (HGA) movements.

[10] In the Gauss co-moving frame.

We refer to Iafolla et al. (2004) for the details of the mathematical derivation of such equations; here we only remind that these accelerations have been obtained in the hypothesis that the angular rate and angular acceleration have only a component along the rotation axis of the MPO, respectively $\omega_0$ and $\dot{\omega}_0$,[11] and that the spacecraft COM has been assumed fixed in its nominal position.

The subscript PSE in Eq. 8 refers to pseudo-sinusoidal errors. Indeed, the contribution from the gravity gradients and that from the inertial accelerations are modulated by the orbital eccentricity $e$ of the MPO around Mercury. Hence, besides the main effect at the orbital period of the MPO (about 8355 s), we have the contribution from the higher order harmonics coming from a Fourier series of the mean anomaly $M$ with coefficients depending from higher powers of the satellite eccentricity, as shown in Eq. 8, up to order $e^2$. Moreover, the solution described by Eq. 8, represents a nominal solution. In fact, it does not consider the additional effects along each axis of the ISA accelerometer that arise from the angular rate and angular acceleration corrections that are necessary in order to guarantee the nadir pointing of the MPO spacecraft. Such effects have been introduced in Sect. 5 where we considered the error budget contribution from the random-like noise.

As described in Iafolla et al. (2004), each vector $\vec{R}_\varsigma$ is the sum of two time-independent vectors and of two time-dependent vectors (hereinafter we drop the subscript ($\varsigma = X, Y, Z$))

$$\vec{R} = \vec{R}_0 \pm \Delta\vec{R}_0 + \vec{R}_t \pm \Delta\vec{R}_t(t) \tag{9}$$

The first contribution $\vec{R}_0$, i.e., a piece of the time-independent part, has been used to define the position-matrix of the accelerometer as shown in Fig. 2 (i.e., $R_0$ represents the nominal reference position of each sensitive element with respect to the spacecraft COM). The vector $\vec{R}_t(t)$ represents the spacecraft COM displacements due to the fuel consumption and sloshing and the HGA movements. This vector plays a significant role in the estimate of the angular rate and angular acceleration constraints and will be described in Sect. 5. The terms $\Delta\vec{R}_0$ (a piece of the time-independent part) and $\Delta\vec{R}_t$ (a piece of the time-dependent part) have been used to define the knowledge of the accelerometer position-matrix. The time-dependent error is very subtle. It has both a deterministic part (mainly due to the periodic movements of the HGA), which is responsible of a periodic error of systematic type, and a stochastic part due to the fuel sloshing, the HGA itself and other random effects.

We are interested in the knowledge of the analysed disturbing effects in order to remove them a posteriori from the accelerometer measurements. In fact, the quantities $\vec{R}_0$ and $\vec{R}_t(t)$ are responsible of these disturbing systematic effects.

For ISA position-and-error matrix we found:

$$\begin{pmatrix} \vec{R}_{0X} \\ \vec{R}_{0Y} \\ \vec{R}_{0Z} \end{pmatrix} \pm \begin{pmatrix} \Delta\vec{R}_{0X} + \Delta\vec{R}_{tX} \\ \Delta\vec{R}_{0Y} + \Delta\vec{R}_{tY} \\ \Delta\vec{R}_{0Z} + \Delta\vec{R}_{tZ} \end{pmatrix} = \begin{pmatrix} 0 & 0 & +5\cdot 10^{-2} \\ 0 & 0 & -5\cdot 10^{-2} \\ 0 & 0 & 0 \end{pmatrix} + \begin{pmatrix} \pm 5\cdot 10^{-3} & \pm 7.5\cdot 10^{-3} & \pm 15\cdot 10^{-3} \\ \pm 5\cdot 10^{-3} & \pm 7.5\cdot 10^{-3} & \pm 15\cdot 10^{-3} \\ \pm 5\cdot 10^{-3} & \pm 7.5\cdot 10^{-3} & \pm 15\cdot 10^{-3} \end{pmatrix} \tag{10}$$

[11] In Eq. 8 the contribution of the gravity gradients is mixed with that due to the centripetal acceleration and the one coming from the angular acceleration: all of them are proportional to $n^2$.

where all the positions and displacements are in meters.[12] The arguments that have produced such values for the positions of ISA sensitive elements and their displacement-errors are fully described in Iafolla et al. (2004).

## 4 Periodic effects and ISA error budget

As underlined in Sect. 2, we are interested in the estimate of the impact of the main disturbing effects on the accelerometer measurements during a typical orbit determination analysis. We have seen that, on the average, the arc length is about 8 h. With regard to the periodic effects contribution, we have to take into account the following disturbing effects: (i) the *thermal effects*; (ii) the *components coupling*; (iii) the *gravity gradients*; and (iv) the *inertial forces*. All of them are responsible of disturbing effects at the MPO mean anomaly $M$ frequency or at higher orders, as in the case of the nominal effects. Our goal is to verify if the sum of their absolute values[13] is below the accelerometer accuracy $A_o$ (about $9.8 \cdot 10^{-9}$).

The displacement-errors, estimated in Iafolla et al. (2004), defining the knowledge of the position-matrix of the ISA accelerometer (Eq. 10), are, respectively, $\Delta X = \pm 5$ mm, $\Delta Y = \pm 7.5$ mm and $\Delta Z = \pm 15$ mm, for each sensitive element of the accelerometer. As we have seen, these errors are the sum of the contribution of both the time-independent and time-dependent parts, $\Delta \vec{R}_0$ and $\Delta \vec{R}_t$, and must be considered as the resultant of the errors in the location of the sensitive elements inside the accelerometer box, plus the errors in positioning this box on the spacecraft mounting plate, plus the errors in the knowledge of the spacecraft COM position because of the fuel consumption and sloshing and the HGA movements. In particular, the HGA will be constantly pointed toward the Earth, while the spacecraft will be nadir pointed toward the centre of Mercury.

These displacement-errors have been (conservatively) estimated assuming that the peak values of the nominal effects were always effective during one orbital revolution of the MPO and that the contribution of the time-independent part and the time-dependent part was equally distributed between them. In other words, in order to estimate the displacement-errors the peak values of the gravity gradients and of the inertial accelerations were compared with $A_o$ (for each axis of the accelerometer). In Iafolla et al. (2004), we estimated that the major constraint was in the radial component of the displacement-error, with a contribution $\Delta X_0 \approx 4$ mm from the time-independent part and a contribution $\Delta X_t \approx 1$ mm from the time-dependent part.[14] The errors along the transversal and out-of-plane directions are less demanding and have been relaxed to the values previously introduced.

Our point here is to verify if the resultant error budget due to the nominal effects (which represents the bulk of the periodic effects contribution to the ISA error budget) is compatible with the contribution of the other periodic effects, in particular with the thermal effects at the MPO orbital period.

Let us analyse each of the previously cited effects at the MPO orbital period.

[12] In Eq. 10, we have not yet considered the contribution from the time-dependent displacements of the spacecraft COM that gives a direct contribution in terms of its second derivative. We refer to Sect. 5 for their contribution.

[13] That is we assumed correlated their disturbing effects.

[14] We are considering only the deterministic part of the time-dependent error.

### 4.1 Thermal effects

The amplitude of these thermal effects on the MPO has been estimated to be about 2°C (see ESA 2004a).

In Sect. 2, we have introduced the thermal stability of the ISA accelerometer and the current attenuation factor obtained by the experimental activity (that we conservatively assumed representative of the ISA active thermal control). Therefore, for the thermal perturbations at the MPO orbital period[15] we obtain a residual effect on the accelerometer axes with an amplitude of about:

$$A_{\text{ther}}|_{\text{SP}} \approx 2^{\circ}\text{C} \cdot 5 \cdot 10^{-7}\,\text{m/s}^2/^{\circ}\text{C} \cdot \frac{1}{700} = 1.4 \cdot 10^{-9}\,\text{m/s}^2 \tag{11}$$

This value corresponds to about 14.6% of the accelerometer accuracy $A_{\text{o}}$.

### 4.2 Components coupling

With the term *components coupling* previously introduced, we mean the contribution of the error $\Delta\alpha$ (at the orbital period) of the time-independent misalignment angle of the accelerometer with respect to the MPO body-fixed reference frame.[16] This error has been estimated to be about 1/3000 radians. Because the largest non-gravitational acceleration at the MPO orbital period is due to the direct solar radiation pressure, and its maximum value has been estimated to be about $10^{-6}\,\text{m/s}^2$ (see Lucchesi and Iafolla 2006), for the misalignment angle[17] we can estimate a maximum contribution of about:

$$A_{\text{mis-angle}}\big|_{\text{SP}} \approx 1 \cdot 10^{-6}\,\text{m/s}^2 \cdot \frac{1}{3000} = 3.3 \cdot 10^{-10}\,\text{m/s}^2 \tag{12}$$

This value corresponds to about 3.4% of the accelerometer accuracy $A_{\text{o}}$. Because the resultant contribution of the analysed periodic errors is about 18% of the accelerometer accuracy, we must be confident that the contribution from the nominal errors be always smaller than $\sim 82\% A_0$.

### 4.3 Nominal effects

From Eq. 8 we can see why the major constraints in the displacement-errors come from the radial direction and in particular for the sensitive element along the radial direction. The constant term $3 + 5e^2 (\approx 3)$, which enters in the expression of the $X$-element, becomes effective only when the spacecraft COM movements are considered (it multiplies the displacement-error $\Delta X_t$). Therefore, this term has played no role in the determination of the ISA position-matrix, but it is significant in the determination of its knowledge as well as in constraining the angular rate and angular acceleration corrections (Sect. 5).

In the case of the $Z$-element the constant term is $1 + \frac{3}{2}e^2\ (\approx 1)$, while in the case of the $Y$-element the constant term is $\frac{1}{2}e^2$ (i.e., negligible). Therefore, only the $Z$-element (i.e., the one with sensitive axis along the MPO rotation axis) will be competitive with the $X$-element (i.e., the one with sensitive axis along the radial direction) in the

[15] These are short-period effects compared with the long-period effects described in Sect. 2.

[16] In practice with respect to the onboard star-tracker.

[17] It will be one of the objectives of ISA inflight calibration to verify, if possible, the alignment of the proof-masses sensitive axes with respect to the MPO principal axes of inertia.

determination of the ISA error budget with regard to the nominal pseudo-sinusoidal effects.

In particular, because the errors from the time-dependent part $\Delta Z_t$ are confined to a mm or a few mm level, the main contribution is due to the time-independent term $\Delta Z_0$, up to $\sim$1 cm (see the discussion in Iafolla et al. (2004)). The larger value for the time-independent displacement-error is then responsible for a contribution of the $Z$-element with an acceleration comparable (both in magnitude and in its periodic behaviour) to that of the $X$-element.

We have performed several simulations of the nominal effects behaviour over one orbital revolution of the MPO around Mercury. In the simulations we have varied the values of the displacement errors $\Delta R_0$ and $\Delta R_t(t)$ inside the limits that we have already discussed. The results are always consistent with an error budget from the pseudo-sinusoidal terms (gravity gradients and inertial accelerations) well below the limit previously obtained of about 82% of the accelerometer accuracy $A_0$, for each axis of the accelerometer. In this error budget we also included the acceleration error due to the deterministic part of the time-dependent errors of the spacecraft COM movements described by $\Delta\vec{R}_t(t)$. This error varies, following our requirements, between 5% and 20% of the measurement error. In particular, over one orbital period of the MPO around Mercury, the average error budget due to the pseudo-sinusoidal terms is below 50% of the accelerometer measurement error $A_0$ in the case of the two proof-masses with sensitive axis along the radial and out-of-plane directions, and less than 10% of $A_0$ in the case of the proof-mass with sensitive axis along the transversal direction.

In Fig. 3 are shown the results of one of the simulations obtained imposing the following conservative requirements (in mm) for the displacement-errors: $\Delta\vec{R}_0 = (4, 5.5, 11)$ and $\Delta\vec{R}_t(t) = (1, 2, 4)$. As we can see, what we anticipated with the previous discussion is confirmed by the simulation: the magnitude and behaviour of the accelerations of the sensitive elements with sensitive axis along the radial direction (solid line) and along the MPO rotation axis (dot line) are comparable and are the largest ones, while the contribution of the acceleration of the sensitive element with sensitive axis along the transversal direction (dashed line) is always smaller (or much smaller) than the previous two contributions.

As we can see the magnitude of the along-track component of the nominal effects (the plus sign curve in Fig. 3) is always smaller than the limit previously determined and the behaviour of the along-track component is very close to that of the transversal component.

Finally, in Figs. 4 and 5 are shown, respectively, the contribution of the time-independent and time-dependent displacement-errors to the analysed nominal effects. From these two Figures we explicitly see that the transversal component of the pseudo-sinusoidal terms is mainly influenced by the time-independent displacement-errors because of their larger values with respect to the time-dependent displacement-errors.

In Table 2, we reassumed our error budget for the periodic effects here analysed. In this Table we have also specified the main parameters which enter in the analysed effects (i.e., we have specified the main parameter(s) which cause the disturbing effect and the main parameter(s) on which the effect imposes a requirement). Because the analysed effects couple each other at the MPO orbital period and mix up, we can, a posteriori, consider such effects as correlated and add their contribution as a sum of their absolute values. The resultant error is about 100% of the accelerometer accuracy.

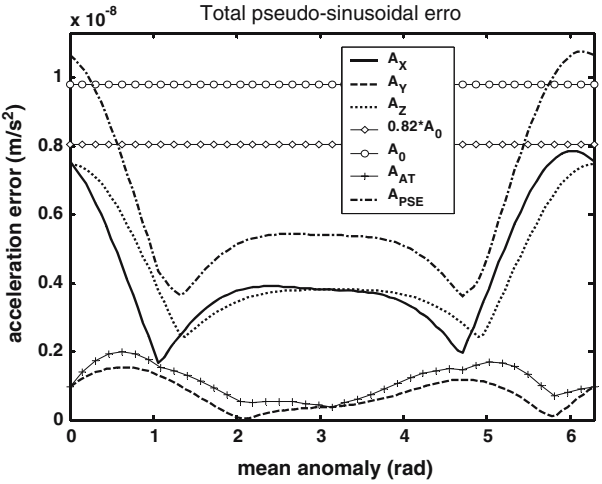


**Fig. 3** Resultant disturbing accelerations on the three axes of ISA due to the gravity gradients and the inertial accelerations (nominal effects or pseudo-sinusoidal terms). The solid line represents the acceleration acting on the $X$-element, the dashed line represents the acceleration acting on the $Y$-element, and finally the dot line represents the acceleration acting on the $Z$-element. The horizontal diamond line represents the limit of $82\%A_0$, while the horizontal circle line represents the accelerometer accuracy $A_0 = 9.8 \cdot 10^{-9}\,\mathrm{m/s^2}$. The dash-dot line represents the absolute value of the disturbing acceleration, while the plus-sign line represents its along-track component. The behaviour of the accelerations over one orbital period of the MPO has been obtained with the following values for the displacement-errors: $\Delta\vec{R}_0 = (4, 5.5, 11)$ mm for the time-independent part and $\Delta\vec{R}_t(t) = (1, 2, 4)$ mm for the time-dependent part. The average error over one orbital revolution of the MPO is below 50% of $A_0$ in the case of the $X$ and $Z$ sensitive elements, while, in the case of the $Y$-element, the average error is less than 10% of the accuracy

In conclusion, the main contribution to the ISA error budget from the periodic effects comes from the *nominal* (or *pseudo-sinusoidal*) effects due to the gravity-gradients, the inertial accelerations and the spacecraft COM displacements due to the HGA movements, which amount to be less than $80\%A_0$.

## 5 Random effects and ISA error budget

In Sect. 2, we have defined the random errors. These errors come from noise sources which are not characterised by precise frequency dependence, that is to say, they arise from noise sources that are spread inside the accelerometer bandwidth with unknown laws. Among the main contributions to such errors we have: (i) the *inertial forces*, (ii) the *thermal effects*, (iii) the *spacecraft COM movements* due to the HGA and fuel consumption and sloshing, (iv) the *components coupling* and (v) ISA *intrinsic noise*.

We stress, one more time, that the results we are going to obtain for ISA error budget connected with the random like errors are rigorously requested only in the low frequency part of the accelerometer bandwidth, between $10^{-4}$ Hz and $10^{-3}$ Hz, where we need to fully exploit the accelerometer spectral density $S_0 = 9.8 \cdot 10^{-9}\,\mathrm{m/s^2}/\sqrt{\mathrm{Hz}}$.

Among the random errors introduced, those from the inertial forces are the most subtle to be considered. They are connected to the sensitive elements stochastic

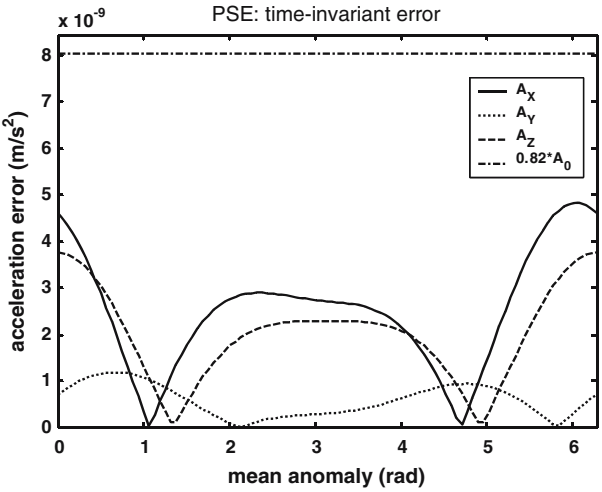


**Fig. 4** Time-independent contribution (with $\Delta\vec{R}_0 = (4, 5.5, 11)$ mm) to the disturbing accelerations on the three axes of ISA due to the gravity gradients and the inertial accelerations (nominal effects). The solid line represents the acceleration acting on the $X$-element, the dot line represents the acceleration acting on the $Y$-element, finally the dashed line represents the acceleration acting on the $Z$-element. The horizontal dash-dot line represents the limit of $82\%A_0$. The average error over one orbital revolution of the MPO is about 25% of $A_0$ in the case of the $X$ and $Z$ sensitive elements, the most sensitive to the pseudo-sinusoidal errors

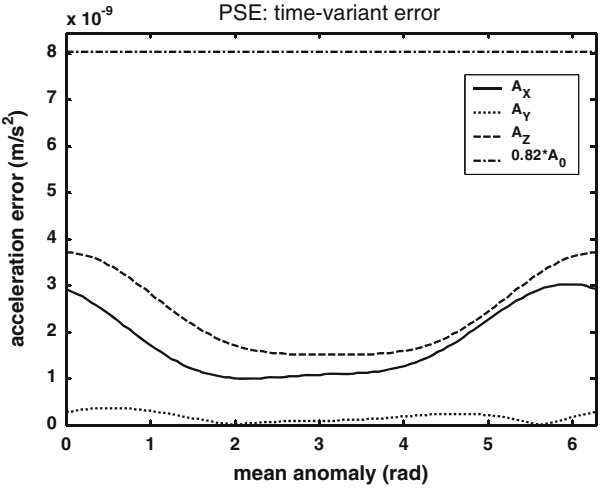


**Fig. 5** Time-dependent contribution (with $\Delta\vec{R}_t(t) = (1, 2, 4)$ mm) to the disturbing accelerations on the three axes of ISA due to the gravity gradients and the inertial accelerations (nominal effects). The solid line represents the acceleration acting on the $X$-element, the dot line represents the acceleration acting on the $Y$-element, finally the dashed line represents the acceleration acting on the $Z$-element. The horizontal dash-dot line represents the limit of $82\%A_0$. The average error over one orbital revolution of the MPO is about 25% of $A_0$ in the case of the $X$ and $Z$ sensitive elements, the most sensitives to the pseudo-sinusoidal errors.

**Table 2** ISA error budget due to the analysed periodic effects

| Perturbing effect | Due to | Spectral contents | Requirement on | Error % $A_0$ |
|---|---|---|---|---|
| Gravity gradients | $n$ | Orbital period $P$ and $P/2$ | $\Delta\vec{R}_0, \Delta\vec{R}_t(t)$ | 80 |
| Inertial forces | $(\omega_0, \dot{\omega}_0)$ | Orbital period $P$ and $P/2$ | | |
| Thermal effects | $\Delta T = 2°\mathrm{C}$ | Orbital period $P$ | $\Delta T$ | 15 |
| Components coupling | $\Delta\alpha = 1/3000$ rad | Orbital period $P$ | $\Delta\alpha$ | 4 |
| Total | | | | 100 |

The most important contributions to the resultant error budget come from the so called *nominal* effects and from the *thermal* effects. The *nominal* effects provide their *grant* at the spacecraft orbital period $P$ (about 8355 s) and at half of the orbital period. The *thermal* effects impact at the MPO orbital period. The *nominal* effects contribution to the error budget includes the acceleration error that comes from the deterministic displacement of the spacecraft COM mainly due to the HGA movements (that we conservatively assumed equal to 20% of $A_0$). The resultant error budget is conservatively obtained adding the absolute values of the analysed errors

displacements with respect to the spacecraft COM and they ultimately impose requirements on the performances of the onboard star-tracker. More precisely, these errors come from the attitude corrections that will be imposed by the MPO star-tracker in such a way to guarantee the nadir pointing of the spacecraft.

In the following, we recall the main results that we obtained on the MPO angular rate and angular acceleration corrections and their contribution to ISA error budget. Then, we compute the error budget from the other random errors (that we do not considered in our previous work) and add together all their contribution.

### 5.1 The MPO angular rate and acceleration constraints and their impact on ISA error budget

Equations 13 and 14 give the deviation from the nominal rotation of the MPO around the out-of-plane direction ($Z$-axis):

$$\vec{\omega} = (\delta\omega_X, \delta\omega_Y, \omega_0 + \delta\omega_Z) \tag{13}$$

$$\dot{\vec{\omega}} = (\delta\dot{\omega}_X, \delta\dot{\omega}_Y, \dot{\omega}_0 + \delta\dot{\omega}_Z) \tag{14}$$

where

$$\omega_0 = \left(1 + 2e\cos M + \frac{5}{2}e^2\cos 2M + O\left(e^2\right)\right) \tag{15}$$

$$\dot{\omega}_0 = n^2\left(-2e\sin M - 5e^2\sin 2M\right) \tag{16}$$

are the nominal angular rate and the nominal angular acceleration necessary for the nadir pointing of the spacecraft. The impact of the additional terms $\delta\omega_\varsigma$ and $\delta\dot{\omega}_\varsigma$ (with $\varsigma = X, Y, Z$) on the accelerometer readings are:

$$\begin{aligned} A_X &\approx 2\omega_0\delta\omega_Z\Delta X_X + \delta\dot{\omega}_Z\Delta X_Y - \omega_0\delta\omega_X\Delta X_Z - \delta\dot{\omega}_Y\Delta X_Z \\ A_Y &\approx -\delta\dot{\omega}_Z\Delta Y_X + 2\omega_0\delta\omega_Z\Delta Y_Y - \omega_0\delta\omega_Y\Delta Y_Z + \delta\dot{\omega}_X\Delta Y_Z \\ A_Z &\approx -\omega_0\delta\omega_X\Delta Z_X + \delta\dot{\omega}_Y\Delta Z_X - \omega_0\delta\omega_Y\Delta Z_Y - \delta\dot{\omega}_X\Delta Z_Y \end{aligned} \tag{17}$$

**Table 3** Requirements in the angular rate and angular acceleration.

| Angular parameter | Requirements |
|---|---|
| $\delta\omega$ | $9 \cdot 10^{-6}$ rad/s/$\sqrt{\text{Hz}}$ |
| $\delta\dot{\omega}$ | $9.4 \cdot 10^{-9}$ rad/s$^2$/$\sqrt{\text{Hz}}$ |

The values reported are the ones we obtained assuming the largest displacements for the spacecraft COM (due to the HGA movements and fuel consumption) with respect to its nominal position. In Iafolla et al. (2004) we estimated the following maximum values for such displacements: about 3 cm along the radial direction, about 2 cm along the transversal direction, about 4 cm along the out-of-plane direction (i.e., along the MPO rotation axis)

where we neglected the contribution of the squared terms in the introduced variations. Of course, these new terms will enrich Eq. 8 of additional contributions.

However, the contribution from $\delta\omega_\varsigma$ and $\delta\dot{\omega}_\varsigma$ can be easily separated from the previous one (pseudo-sinusoidal terms) because of their different spectrum. Therefore, it is enough to estimate their impact with respect to the accelerometer spectral density ($S_0 = 9.8 \cdot 10^{-9}$ m/s$^2$/$\sqrt{\text{Hz}}$) using Eq. 17. The displacements which enter Eq. 17 are those defining the ISA position matrix with respect to the true centre-of-mass of the MPO spacecraft, i.e., $\vec{R}_0$ and $\vec{R}_t$. In fact, we must consider the contribution of both the time-independent part and the time-dependent part of the displacements.

The requirements in the angular rate $\delta\omega_\varsigma$ and in the angular acceleration $\delta\dot{\omega}_\varsigma$ have been estimated in Iafolla et al. (2004). In Table 3 are shown the results obtained in a conservative case.

Such values have been obtained from a worst case analysis where we constrained the disturbing acceleration along each of the three axes of the accelerometer to 60% of ISA spectral density $S_0$. In that analysis we also assumed that each of the four terms of the disturbing acceleration in Eq. 17, contributes with the same weight to the resultant acceleration along each sensitive axis.

In reality, with the approach we developed in ESA (2006) we constrained the disturbing accelerations produced by the random component of the inertial forces to values well below the 60% level of the accelerometer spectral density. In fact, the values shown in Table 3 come from the minimum envelope curves that we obtained (from Eq. 17) for the behaviours of the angular rates and the angular accelerations along each axis of the accelerometer (we refer to ESA (2006) for major details).

Therefore, with the previous arguments we have constrained the contribution to the error budget from the random component of the inertial forces to values smaller than 60% of the accelerometer spectral density $S_0$. Now we need to estimate the contribution to ISA error budget from the other random effects previously introduced.

## 5.2 Thermal effects

In the case of the thermal effects, we assumed the presence of a white like noise at the interface between the MPO structure and the accelerometer box with an amplitude of about 4°C/$\sqrt{\text{Hz}}$. This temperature variation is transformed by the accelerometer in an equivalent acceleration through its thermal stability ($5 \cdot 10^{-7}$ m/s$^2$/°C) and then attenuated by a factor 700 through the accelerometer active thermal control. The resultant acceleration (along each axis) that contributes to the accelerometer readings is:

$$A_{\text{ther}}|_{\text{rand}} \approx 4°\text{C}/\sqrt{\text{Hz}} \cdot 5 \cdot 10^{-7}\ \text{m/s}^2/°\text{C} \cdot \frac{1}{700} = 2.9 \cdot 10^{-9}\ \text{m/s}^2\sqrt{\text{Hz}} \qquad (18)$$

This value corresponds to about 29.6% of the accelerometer spectral density $S_0$.

### 5.3 Movements of the HGA and fuel consumption and sloshing

Let us describe the stochastic like errors that arise from the HGA movements as well as from the fuel consumption and sloshing.[18] These noise sources have a double impact on ISA error budget. From one side they provide a direct contribution to the spacecraft COM displacement, i.e., they impose a requirement on the knowledge of the spacecraft COM acceleration error $\Delta\vec{A}_t$, where $\vec{A}_t$ represents the second derivative of the time-dependent vector $\vec{R}_t$ previously introduced. From the other side they impact as a direct noise on the MPO structure.

We imposed, for each sensitive axis of ISA, the first contribution to be not larger than 70% of the spectral density, while the second to be about 10% of the spectral density. In Figs. 6 and 7 are shown, respectively, the behaviour of the acceleration error of the MPO centre-of-mass displacement and that of the knowledge of the MPO centre-of-mass position that corresponds to that acceleration error. Such results are valid for each sensitive axis of the accelerometer. The acceleration noise has been assumed flat at the value of about $70\%S_0$ between $10^{-4}$ Hz and $10^{-3}$ Hz, then it has been relaxed by a factor of 10 both at lower frequencies ($10^{-5}$ Hz) and at higher frequencies ($10^{-1}$ Hz). In this way the acceleration error follows the constraints imposed on the accelerometer spectral density by the RSE requirements of Fig. 1.

As we can see from Fig. 7, the acceleration error $\Delta A_t = 7 \cdot 10^{-9}\,\mathrm{m/s^2}/\sqrt{\mathrm{Hz}}$ in the $10^{-4}$ to $10^{-3}$ Hz bandwidth, produces a displacement-error $\Delta R_t$ of about $18\,\mathrm{mm}/\sqrt{\mathrm{Hz}}$ at $10^{-4}$ Hz and about $0.2\,\mathrm{mm}/\sqrt{\mathrm{Hz}}$ at $10^{-3}$ Hz (green line).

However, we have already estimated a value for $\Delta\vec{R}_t$ in our previous analysis of the pseudo-sinusoidal errors (that we assumed in the range between 5% and 20% of the measurement error $A_0$ over one orbital period of the MPO). Indeed, as shown in Fig. 5 and explained in Sect. 4, the knowledge of the time-dependent vector was constrained to the values: $\Delta\vec{R}_t = (1, 2, 4)$ mm. This values are midway between those obtained from the acceleration error constraints imposed on the spacecraft COM movements (i.e., from the stochastic contribution) and are valid at the MPO orbital period.

In Fig. 7, we have assumed, as our reference for the requirement on the knowledge of the spacecraft COM position due to the pseudo-sinusoidal error (i.e., the deterministic errors contribution to the spacecraft COM movements) the dashed line at the value of 1 mm (flat at all frequencies).

### 5.4 ISA intrinsic noise

As underlined in Sect. 2, ISA intrinsic noise is at a level of about $9.8 \cdot 10^{-10}\mathrm{m/s^2}/\sqrt{\mathrm{Hz}}$ inside the accelerometer bandwidth ($3 \cdot 10^{-5}$ to $10^{-1}$ Hz). This level corresponds to 10% of the accelerometer spectral density $S_0$. ISA intrinsic noise is limited by the Brownian noise of the oscillator as well as by the amplifier noise. This is shown in Eq. 15 for the square of the accelerometer intrinsic noise:

[18] In Sect. 4, we instead analyzed the systematic contribution to the spacecraft COM displacement due to the deterministic part of the time-dependent error $\Delta R_t$.

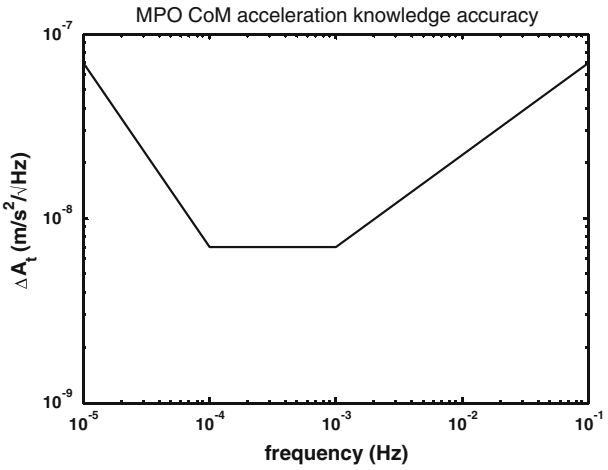


**Fig. 6** Estimate of the acceleration error due to the displacement error of the spacecraft COM variations produced by the HGA movements and by the fuel consumption and sloshing (i.e., from the stochastic errors). This error is connected to the MPO centre-of-mass acceleration noise; it is a linear acceleration and its value is clearly independent from the accelerometer position inside the MPO

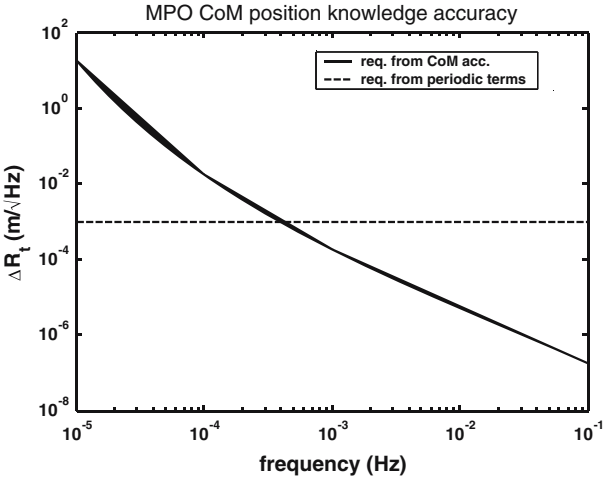


**Fig. 7** Estimate of the knowledge in the MPO centre-of-mass position. The solid line represents the requirement on the knowledge of the spacecraft COM due to the random noise (i.e., from the stochastic errors). The dashed line represents the requirement on the knowledge of the spacecraft COM due to the pseudo-sinusoidal error (i.e., from the deterministic errors that we analyzed in Sect. 4)

$$a_{\mathrm{IN}}^2(f) \cong 8\pi \frac{k_{\mathrm{B}} f_0}{m\Delta t}\left(\frac{T}{Q} + 8\pi T_{\mathrm{n}} \frac{Z_{\mathrm{n}} C f_0}{\beta}\right) \tag{19}$$

where the first term represents the Brownian noise while the second term the amplifier noise. The quantities $f_0$, $k_{\mathrm{B}}, m$ and $\Delta t$ are, respectively, the oscillator resonance frequency (about 3.5 Hz), Boltzmann constant, the mass of the sensitive element and the acquisition time. Then, $T$ and $Q$ are the oscillator absolute temperature and quality factor (comprehensive of the dissipation in the mechanical oscillator and of the

thermal noise associated with the transducer losses); $\beta$ represents the electromechanical factor, $T_n$ and $Z_n$ are, respectively, the amplifier temperature noise and impedance noise; finally $C$ represents the capacitance of the capacitor for the signal extraction. In conclusion, the main limitation in the precision of the measurements is not connected with the accelerometer intrinsic noise but with the noise level present on the spacecraft. We refer to Iafolla and Nozzoli (2001) for major details of ISA physical characteristics.

### 5.5 Components coupling

With regard to the components coupling, as in the case of the periodic effects, their contribution comes from the misalignment angle of the accelerometer with respect to the MPO star-tracker produced by the random-like noise. Its contribution is negligible with respect to the accelerometer spectral density. Indeed, a typical star-tracker gives an error $\delta\alpha$ of about $5 \cdot 10^{-6}\,\mathrm{rad}/\sqrt{\mathrm{Hz}}$ (see ESA 2004b).

Following the same arguments described in Sect. 4, such value for the random component of the misalignment angle corresponds to an equivalent acceleration noise of about $5 \cdot 10^{-12}\,\mathrm{m/s^2}/\sqrt{\mathrm{Hz}}$ at 1 Hz. This very small noise is further reduced, by at least three orders-of-magnitude, integrating inside the narrower bandwidth $10^{-4}$ to $10^{-3}$ Hz.

In Table 4, we reassumed the results here described for the random noise contribution to the accelerometer error budget, including ISA intrinsic noise and the negligible effects due to the components coupling. As in the case of the periodic effects, in this Table we have also specified the main parameters which enter in the definition of the described effects. Because the analysed disturbing effects are not correlated, we added their contribution in a root-sum-square fashion. We like to note that the test masses are made using a non-ferromagnetic material and in the pick-up signal scheme they are electrical grounded, ensuring that the Lorentz forces give a negligible contribution.

**Table 4** ISA error budget due to the random noise

| Perturbing effect | Due to | Spectral contents | Requirement on | Error $\%A_0$ |
|---|---|---|---|---|
| Inertial forces | $\vec{R}_0, \vec{R}_t(t)$ | Random | $\delta\omega, \delta\dot{\omega}$ | 60 |
| Thermal effects | $\Delta T = 4°\mathrm{C}/\sqrt{\mathrm{Hz}}$ | Random | $\Delta T$ | 30 |
| MPO COM displacement | Movements HGA,... | Random | $\Delta\vec{A}_t(t)$ | 70 |
| Noise on the MPO | Movements HGA, ... | Random | | 10 |
| ISA intrinsic noise | Mechanical oscillator | Random | Mech. and Elect, par. | 10 |
| Components coupling | $\delta\alpha \cong 5 \cdot 10^{-6}$ rad/$\sqrt{\mathrm{Hz}}$ | Random | $\delta\alpha$ | Negligible |
| Total (not correlated noise) | | | | 100 |

The main contribution to the error budget comes from the spacecraft COM displacements due to the HGA movements and to the fuel consumption. The resultant error budget is obtained as the root-sum-square of the described error sources

## 6 Conclusions, recommendations and future work

In this paper we have focused on a preliminary estimate for the error budget of the ISA accelerometer onboard the MPO spacecraft of the BepiColombo space mission to Mercury. In particular, we have subdivided the errors into two main families: (i) the periodic errors and (ii) the random errors. We fixed requirements to the satellite in order to constrain the magnitude of the error sources to a fraction of the accelerometer accuracy $A_o$ and spectral density $S_o$.

Both definitions are a measure of the accelerometer measurement error, the first matches directly with the ISA measurement error over the typical arc length during the MPO orbit determination (i.e., with the RSE mission accuracy), the second is more suitable to be used when the error sources are characterised by a noise-like spectrum. The main results achieved with this work can be summarised as follows:

(1) among the systematic (i.e., deterministic) errors the main perturbations are connected to the *nominal* effects produced by Mercury's gravity gradients and by the *inertial forces* which are present on the rotating MPO spacecraft, as well as by the *thermal effects* at the spacecraft orbital period (Sects. 3 and 4), see Table 2;
(2) the nominal effects have been also defined as pseudo-sinusoidal effects because they impact on the accelerometer measurements with the mean anomaly frequency (i.e., at the MPO orbital period of about 8355 s) but also with its higher order harmonics and with coefficients depending on higher powers of the MPO orbit eccentricity $e$;
(3) the nominal effects impose a requirement on the knowledge of the displacement-errors produced by both the time-independent part and the time-dependent part of the accelerometer sensitive elements position with respect to the (true) COM of the spacecraft. We have proved that if the sum of such displacement-errors is confined (for each sensitive element) to the values 5, 7.5 and 15 mm, respectively along the radial direction, the transversal direction and along the out-of-plane direction, the error budget from the pseudo-sinusoidal terms is always smaller than 80% of the accelerometer accuracy (see Fig. 3);
(4) with regard to the thermal disturbing effects at the MPO orbital period, we have seen that with an active thermal control we will be able to attenuate their effect by a factor 700, reducing their contribution to ISA error budget around 15% of the accelerometer accuracy. These effects impose a requirement on the temperature variation (at the MPO orbital period of about 8355 s) $\Delta T$ on the ISA structure, presently estimated around 2°C (Sect. 4);
(5) in the case of the random-like errors the main perturbations are produced by the spacecraft *COM displacements,* by the *thermal effects* and by the deviation from the nominal rotation of the MPO (i.e., by the *inertial forces)*, see Sect. 5 and Table 4;
(6) the spacecraft COM displacements are mainly due to the onboard HGA movements and to the fuel consumption. We have fixed their impact on the accelerometer readings to 70% of ISA spectral density imposing a requirement in the knowledge of the spacecraft COM acceleration error $\Delta\vec{A}_t$, see Figs. 6, 7;
(7) the possible thermal effects with a random-like behaviour are abated by the accelerometer active thermal control. They have been confined to a value around 30% of ISA spectral density with the suggested active thermal control;

(8) the random errors related with the inertial forces are the most subtle to deal with. They come from the star-tracker attitude corrections that are necessary to guarantee the nadir pointing of the MPO spacecraft. They impose requirements on the knowledge of the angular rate $\delta\omega$ and angular acceleration $\delta\dot{\omega}$ corrections and are connected with the ISA sensitive elements position with respect to the (true) centre-of-mass of the spacecraft. For the values shown in Table 3 for the angular rate and acceleration corrections, the impact of these effects on the accelerometer measurements will be much smaller than our initial estimate of about 60% of ISA spectral density, see Table 4.

Most of the consequences of this work rely on the assumptions we made on the knowledge of the ISA position-matrix and on the requirements imposed by the accelerometer performances on the knowledge of the onboard star-tracker corrections for the requested nadir pointing of the spacecraft. The final solutions for such parameters (e.g., positions knowledge and angular rates and angular accelerations knowledge) will be imposed (following our requirements) by the industrial contractor that will be in charge of the MPO construction and of the ISA implementation onboard the spacecraft.

Anyway, we have based our analyses on feasible arguments and also on conservative assumptions. Therefore, we believe practicable our requirements and consequently our error budget results for the analysed periodic and random errors (that we conservatively consider a preliminary estimate).

A very important issue is related, once in orbit around Mercury, with the accelerometer calibration. A forthcoming paper will be devoted to our preliminary analysis of the inflight calibration procedures for ISA, with particular emphasis on the measurement of the proof-masses transducer factor and of their centre-of-mass position with respect to the spacecraft effective COM.

The ongoing NASA mission to Mercury denominated MESSENGER (see for instance Solomon et al. 2001) is complementary to BepiColombo and is characterised by different orbital parameters. Among the several instruments onboard the MESSENGER spacecraft, an HGA and a transponder will be devoted to RSE. However, MESSENGER has not an onboard accelerometer and has not a multi-frequency coherent link as BepiColombo.

We stress that the opportunity of an onboard accelerometer, together with the high performances of the multi-frequency coherent link (both in range and range-rate), will give to the BepiColombo RSE the necessary final accuracy in order to reach its very ambitious goals.

**Acknowledgements** The authors are grateful to A. Milani (Pisa University, Italy), A. Rossi (ISTI/CNR, Italy) and to L. Iess (Roma University "La Sapienza", Italy) for providing input for this research and to R. Peron (IFSI/INAF, Roma, Italy). D.L. is also grateful to the staff of the Space-Flight Dynamics Laboratory for kind hospitality at ISTI/CNR during these years. Special thanks to the two anonymous reviewers. Their remarks and suggestions have considerably improved the paper with respect to the original one.

## References

Colombo, G.: Rotational period of the planet Mercury. Nature **208**, 575 (1965)
Colombo, G.: Cassini's second and third laws. Astron J. **71**, 891 (1966)
Colombo, G., Shapiro, I.I.: The rotation of the placet Mercury. Astrophys. J. **145**, 296 (1966)

ESA document SCI-PB/RS/1140, 2004a. Experiment Interface Document. Part A. SCI-PB/RS/1140, 1 March 2004
ESA document SCI-A/2002/007/Dc/CE, CR_BC_TN15, 2004b. BepiColombo Payload Study Document. SCI-A/2002/007/Dc/CE, CR_BC_TN15, 19 February 2004
ESA document BC-EST-RS-02520-Draft-01, 2006. ISA Experiment Interface Document Part B Document BC-EST-RS-02520-Draft-01, 9 February 2006
Grard, R., Balogh, A.: Returns to Mercury: science and mission objectives. Plan. Space Sci. **49**, 1395–1407 (2001)
Iafolla, V., Nozzoli, S.: Italian spring accelerometer (ISA) a high sensitive accelerometer for "Bepi-Colombo" ESA CORNERSTONE. Plan. Space Sci. **49**, 1609–1617 (2001)
Iafolla, V., Lucchesi, D.M., Fiorenza, E., Nozzoli, S.: Scientific and technological plan, Annex_3: ISA positioning inside the MPO, IFSI INAF internal report, 12 May 2004
Iess, L., Boscagli, C.: Advanced radio science instrumentation for the mission BepiColombo to Mercury. Plan. Space Sci. **49**, 1597–1608 (2001)
Lucchesi, D.M., Iafolla, V.: The non-gravitational perturbations impact on the BepiColombo radio science experiment and the key role of the ISA accelerometer: direct solar radiation and albedo effects. Celest. Mech. Dyn. Astron. **96**, 99–127 (2006)
Milani, A., Rossi, A., Vokrouhlick, D., Villani, D., Bonanno, C.: Gravity field and rotation state of Mercury from the BepiColombo Radio Science Experiments. Plan. Space Sci. **49**, 1579–1596 (2001)
Milani, A, Vokrouhlicky, D., Villani, D., Bonanno, C., Rossi, A.: Testing general relativity with the Bepicolombo radio science experiment. Phys. Rev. D. **66**, 082001 (2002)
Solomon, S.C., McNutt, R.L., Gold, R.E.: The MESSENGER mission to Mercury: scientific objectives and implementation. Plan. Space Set. **49**, 1445–1465 (2001)
Spohn, T., Sohl, F., Wieczerkowski, K., Conzelmann, V.: The interior structure of Mercury: what we know, what we expect from BepiColombo. Plan. Space Sci. **49**, 1561–1570 (2001)